Published in final edited form as:
Soft Matter. 2010 July 21; 6(14): 3232–3236. doi:10.1039/C002632H.

Viscosity and interfacial properties in a mussel-inspired adhesive coacervate†

Dong Soo Hwang[‡,a], **Hongbo Zeng**[‡,b,c], **Aasheesh Srivastava**[a], **Daniel V. Krogstad**[a], **Matthew Tirrell**[a,b,d], **Jacob N. Israelachvili**[a,b], and **J. Herbert Waite**[e]

[a]Materials Research Laboratory, University of California, Santa Barbara, California, 93106, USA. dshwang@mrl.ucsb.edu; Fax: +1-805-893-7998; Tel: +1-805-893-5787

[b]Department of Chemical Engineering, University of California, Santa Barbara, California, 93106, USA. hongbo.zeng@ualberta.ca; Fax: +1-780-492-2881; Tel: +1-780-492-1044

[c]Department of Chemical and Materials Engineering, University of Alberta, Edmonton, Alberta, T6G 2V4, Canada

[d]Departments of Bioengineering, Chemical Engineering and Materials Science & Engineering, Materials Science Division, Lawrence Berkeley Laboratory, University of California, Berkeley, CA, 94720-1762, USA

[e]Department of Molecular, Cell, and Developmental Biology, University of California, Santa Barbara, California, 93106, USA

Abstract

The chemistry of mussel adhesion has commanded the focus of much recent research activity on wet adhesion. By comparison, the equally critical adhesive processing by marine organisms has been little examined. Using a mussel-inspired coacervate formed by mixing a recombinant mussel adhesive protein (fp-151-RGD) with hyaluronic acid (HA), we have examined the nanostructure, viscosity, friction, and interfacial energy of fluid-fluid phase-separated coacervates using the surface forces apparatus and microscopic techniques. At mixing ratios of fp-151-RGD:HA resulting in marginal coacervation, the coacervates showed shear-thickening viscosity and no structure by cryo-transmission electron microscopy (cryo-TEM). However, at the mixing ratio producing maximum coacervation, the coacervate showed shear-thinning viscosity and a transition to a bicontinuous phase by cryo-TEM. The shear-thinning viscosity, high friction coefficient (>1.2), and low interfacial energy (<1 mJ m^{-2}) observed at the optimal mixing ratio for coacervation are promising delivery, spreading and adhesion properties for future wet adhesive and coating technologies.

Introduction

Achieving and maintaining strong adhesion on polar surfaces in the presence of moisture remains a high though elusive technological priority, particularly in medical and dental applications. The detailed analysis of adhesion by sessile marine organisms such as tubeworms and mussels is providing useful insights into the requirements for successful underwater adhesion. One such insight is chemical: the surface-active components of mussel

†Electronic supplementary information (ESI) available: Fig. S1–S3. See DOI: 10.1039/c002632h

Correspondence to: Dong Soo Hwang; Hongbo Zeng.

‡D. S. Hwang and H. Zeng contributed equally to this work

and worm adhesives are proteins rich in 3,4-dihydroxyphenyl-L-alanine (DOPA) – a catecholic amino acid derived from tyrosine.[1] For example, mussel footprint proteins such as mfp-3 and -5 contain between 20–30 mole % DOPA. DOPA's repertory of surface interactions is versatile and includes both covalent and coordination complexes.[2] Increasingly, synthetic polymers are being engineered with catecholic functionalities for robust adhesive and coating applications.[3–5]

A second emerging insight is physical and relates to adhesive processing. All mussel and tubeworm adhesive proteins discovered to date lack secondary structure and have hydrophilic primary sequences with high charge densities (~1 charge per every 5 amino acids);[1] in other words, these proteins are poly-electrolytes. The sandcastle worm adhesive contains roughly equal amounts of both anionic and cationic polyelectrolytes, which have been identified as phosphoserine-rich and lysine-rich proteins, respectively.[6,7]

Secreting highly soluble polyelectrolytes directly into seawater where they will be quickly diluted by diffusion seems counterproductive for adhesion. Aqueous mixtures of oppositely charged polyelectrolytes, however, usually undergo a fluid-fluid phase separation at pH where the mixture has no net charge. This process is called complex coacervation, and the denser, polymer-rich phase is referred to as the coacervate phase.[8,9] Coacervates are used extensively in encapsulation technology[10] and have even been formulated into a bone cement based on mussel- and sandcastle worm-inspired polyelectrolytes with catecholic functionalities.[4]

Complex coacervation for dispensing adhesive proteins seems adaptively beneficial for marine organisms in that a fluidic adhesive can be positioned and spread over a selected surface without loss to the surrounding seawater.[1] Coacervates can accommodate very high protein concentrations without a significant compromise in solute diffusion coefficients,[11,12] and, by oxidizing DOPA, coacervates can be cured or transformed into solids.[4] Indeed, mussel-inspired coacervates show a distinct potential as coatings for medical implant materials.[13]

In this report, with the aid of a surface forces apparatus (SFA) we examined the viscosity, frictional coefficient, and interfacial energy of a coacervate prepared by the complex coacervation of a cationic recombinant mussel adhesive protein (fp-151-RGD) and hyaluronic acid (HA) that showed potential for medical implant coating materials (Fig. S1†).[13] How a coacervate flows during microfluidic delivery from the adhesive glands to the surface, and how readily it spreads once applied to a surface underwater are as crucial to understanding the biology as they are for developing rationally designed new adhesive technologies.

Experimental

Materials

Hyaluronic acid (MW_{AV} = 35,000) was purchased from Lifecore (Chaska, MN, USA) and recombinant mussel adhesive protein, fp-151-RGD (MW = 25,100), was generously donated by Kollodis Biosciences, Inc (MA, USA). The sequence of fp-151-RGD was previously reported[14] and basically consists of an mfp-5 sequence sandwiched between two domains each consisting of 6 repeats of the decapeptide AKPSYPPTYK from mfp-1. RGD denotes a short cell binding sequence which does not pertain to the present study. DOPA-containing fp-151-RGD was prepared from fp-151-RGD using mushroom tyrosinase to hydroxylate tyrosyl residues.[15]

Complex coacervation of HA and fp-151-RGD

Stock solutions of 0.1% (w/v) HA (polyanion) and 0.1% (w/v) fp-151-RGD (polycation) were prepared in 10 mM sodium acetate buffer (pH 5.0). The total polymer concentration was fixed at 0.1% (w/v) for all combinations of HA and fp-151-RGD. Complex coacervation of the two polyelectrolytes was measured turbidimetrically at 600 nm by UV-vis spectrophotometry. fp-151-RGD absorbance was negligible at 600 nm. The relative turbidity is defined as $-\ln(T/T_0)$ where T and T_0 are light transmittance with and without sample, respectively.[13] The turbidity associated with coacervate droplet formation was also visually inspected by inverted light microscopy. The zeta potential of coacervates was measured by a Malvern 3000 Zetasizer instrument at 25 °C. The instrument uses a 10 mW He–Ne laser operating at 632.8 nm. Changes in the zeta potential of complex coacervate of HA/fp-151-RGD were investigated by incremental additions wt% of HA at pH 5.0.

Microscopy

Rhodamine B (RhoB)-labeled fp-151-RGD and 6-aminofluorescein-labeled hyaluronic acid were synthesized as previously described.[11] Polyelectrolyte distribution within the coacervate was investigated by confocal microscopy on a Leica instrument (DMIRBE) with a 63× water-type objective, and double illuminated using Ar (488 nm) and Kr (568 nm) lasers. To minimize the interference between the dyes, the fluorescein emission filter was set between 500 and 540 nm whereas RhoB emission was recorded between 620 and 660 nm. All samples were prepared for cryo transmission electron microscopy (Cryo-TEM) using the environmentally controlled Vitrobot Mark IV from FEI Company. The environmental chamber was heated to 24 °C and 100% humidity. In a typical sample preparation, a 1– 4 μL droplet of the coacervate was pipetted onto a lacey carbon coated copper grid. The sample was then blotted 1–2 times with filter paper for 2–3 s each before being plunged into liquid nitrogen cooled liquid ethane. The samples were placed in a Gatan cryo-holder and were kept below −170 °C. The samples were imaged at 200 kV with an FEI Technai T20 microscope using the low dose imaging mode.

Friction measurement

The lateral (friction) forces of the coacervate were determined using a surface forces apparatus (SFA) configured as previously described.[16,17] Basically, a thin mica sheet of 1–5 μm was glued onto a cylindrical silica disk (radius 2 cm). 50–100 μL of coacervate (1 mg mL^{-1} check this value) was pipetted onto one mica surface. As coacervate micro-droplets coalesced, the condensed coacervate settled onto the mica surface due to its higher density. The settlement effectively separates the dilute water phase from the denser coacervate (see Fig. 1). The two curved mica surfaces were mounted in the SFA chamber in a crossed-cylinder geometry, which roughly corresponds to a sphere of radius Ron a flat surface based on the Derjaguin approximation. The bottom surface was supported by a double cantilever spring, which was connected to a piezoelectric bimorph slider. Lateral (or shear) movement of the bottom surface was accomplished with a bimorph slider, and the friction forces were measured using a “friction device”.[16] All experiments were performed at room temperature (23 °C).

Result and discussion

The surface forces apparatus set-up for measuring the physical properties of the mussel inspired coacervate phase

As commercially available reagent grade HA with a low polydispersity index is relatively expensive and the production and purification of recombinant mussel adhesive proteins are labor-intensive, micro-rheological methods that work with small sample quantities and

volumes (≤ 10 mg, or < 100 μL) are preferred. The surface forces apparatus (SFA) used in our study to monitor the physical properties of the coacervate phase requires very small volumes (~50 μL liquid). The SFA has been used for many years to measure the physical forces for different materials and in various systems, including the lateral and normal forces in complex fluids. In this work, the SFA also allows insights into the wetting and spreading of the coacervate phase on the contacting solid surfaces. The SFA can accurately measure forces as low as 10 nN and surface separations with Ångström resolution by using multiple beam interference fringes of equal chromatic order (FECO).[17] In the following experiments, the dense coacervate phase was formed and confined between two mica surfaces as shown in Fig. 1. The thickness of the confined coacervate phase or the gap distance between the two mica surfaces was monitored in real time using the FECO fringes. The two surfaces were brought together to permit the coacervate fluid film to coalesce and make contact with the opposing mica surface and spread. As the coacervate spread on the second mica surface, it formed a continuous viscous bridge as shown in Fig. 1. The two surfaces were then sheared back and forth by using a piezoelectric bimorph slider with the sliding distance fixed at ~30 μm. Previous study has shown that for the geometry of Fig. 1, the shear or friction force $F_{\|}$ is related to the viscosity η of the liquid between the surfaces by eqn (1a), and shear rate $\dot{\gamma}$ is given by eqn (1b), where R is the radius of curvature and related to cylinder radii R_1 and R_2 by $R^2 = 2(R_1R_2)^{3/2}/(R_1 + R_2)$ (for two crossed cylinders, the common geometry of SFA experiments), $V_{\|}$ is the shear velocity and D is the closest distance of separation[18–20]

$$F_{\|} \approx (16\pi/5)R\eta V_{\|}\ln(2R/D) \tag{1a}$$

$$\dot{\gamma}=\frac{V_{\|}}{D} \tag{1b}$$

Both the FECO fringes and microscopic top-views were continuously video-recorded during the experiment. As a rule, FECO patterns were smooth and continuous when the liquid phase trapped in the gap between two mica surfaces was homogeneous (Fig. 1), whereas when the aqueous phase was heterogeneous, FECO displayed discontinuities due to changes in the local refractive index and film roughness.[21]

Characterization of the micro- and nano-structure of the coacervate phase

Except for the buffer pH (10 mM sodium acetate, pH 5.0), coacervation of HA and fp-151-RGD was performed as previously described.[13] Turbidity levels in the different HA:fp-151-RGD mixtures provide a quantitative measure of the coacervate yield. Five different mixing ratios (HA: fp-151-RGD = 0 : 1, 1 : 9, 1 : 3, 2 : 3, 1 : 0) were selected to assess the correlation of coacervate physical properties with the degree of yield and charge neutralization (Fig. 2). After labeling with fluorescence dyes (FITC for HA and Rhodamine B for fp-151-RGD), the distribution of each polymer within the coacervate was scrutinized by confocal microscopy. Since FITC and Rhodamine B fluorescence appeared uniform throughout the coacervate, we conclude that HA and fp-151-RGD are distributed with similar uniformity within the coacervate in agreement with a previous confocal investigation (Fig. 3).[11] Coacervates resulting from the different mixing ratios in Fig. 2 were inspected by cryotransmission electron microscopy. The coacervate produced from the 1 : 3 ratio (HA: fp-151-RGD) has a tubular network with diameters ranging from 10–20 nm (Fig. 4). Comparable structures could not be detected in coacervates formed at any of the suboptimal mixing ratios (1 : 9 and 2 : 3)

Some physical properties of the mussel inspired coacervate phase by SFA

The coacervates were allowed to settle on the mica surfaces before studying their physical properties *via* the SFA. Upon settling, coacervates resemble polymer melts. Polymer concentration in coacervates is quite high. Based on the coacervate volume applied to the mica surfaces (by FECO) and by amino acid analysis of the HA and fp-151-RGD-depleted equilibrium phase, polyelectrolyte concentration in the coacervate (HA:fp-151-RCD 1 : 3) was estimated to be ~500 mg mL^{-1}, which is 500 times higher than the HA and fp-151-RGD solute concentrations (1 mg mL^{-1}) preceding coacervation.

After allowing the settled coacervate phase to bridge and spread over both mica surfaces, a lateral shearing force was applied between the surfaces. To avoid effects of strong confinement, which might arise in a very narrow gap (see ESI, Fig. S2†), viscosities of the coacervate phases were measured over fixed 100 nm gap distances. At HA:fp-151-RGD ratios of 1 : 9 and 2 : 3 at which coacervation has a substantial charge imbalance, coacervates between mica surfaces behaved as a shear thickening fluid (Fig. 5a and c). In stark contrast, at an HA:fp-151-RGD ratio of 1 : 3, where coacervation is optimal, the coacervate behaved as a shear thinning fluid (Fig. 5b). Functionalization of fp-151-RGD with DOPA (~13 mole %) did not significantly alter the trends in viscosity (Fig. 5d, e, and f). Viscosities of fp-151-RGD and HA (100mg mL^{-1}) measured by SFA show slight shear thinning within the range of shear rates tested (Fig. S3†).

The interfacial energy of the coacervate–water interface can be experimentally determined by SFA. The effective interfacial energy (γ_{eff}) was calculated using $g_{eff} = F_t/4pR$

$$\gamma_{eff} = F_{\perp}/4\pi R \tag{2}$$

where $F_{\perp}$ is the pulling force and R is the radius of curvature. γ_{eff} was found to fall between 0.6–3.0 mJ m^{-2} depending on the pulling force rate (2–20 μN s^{-1}). The thermal equilibrium interfacial energy is estimated to be <1 mJ m^{-2}.

The load dependence of the shear (friction) force was also measured (Fig. 6) and gives a friction coefficient of 1.2–1.4 for all combinations of the polyelectrolytes. The high friction coefficient appears to be independent of coacervation suggesting that the macromolecules secreted from mussel feet and other organisms could prevent slippage at any mixing ratio during holdfast formation.

To better appreciate the biology of adhesive processing and with an eye toward capturing useful insights for improving the technology of wet adhesion, we measured the viscosity of various HA and fp-151-RGD mixing ratios at different shear rates. All of these changing properties correlate nicely with each other and with previous trends observed in coacervates.[22] Thus, as the mole fraction of negatively charged HA is progressively increased we expect the surface charge density of the coacervate-solution interface to first decrease (become less positive as the positive charge of fp-151-RGD is neutralized) then increase as the interface becomes more negative. As zero net charge is approached (from either end) the droplet curvature is expected to decrease causing the coacervate droplets to grow and coalesce into larger and/or more interconnected, such as bicontinuous, lamellar or " sponge phase", structures,[22,23] as observed here (Fig. 4). And both the turbidity and the viscosity are also expected to exhibit the greatest changes in this region,[9,23] as observed here (Fig. 2 and 5).

These results have intriguing biological implications. During secretion of adhesive, the protein mixture passes from the cells to a conducting tubule with a diameter of ~40–60 μm

and is finally dispensed through pores having a diameter of 20–30 μm.[24,25] As the shear rate at fixed volume flow rate increases with the inverse cube of the diameter, a halving of the diameter would increase the shear rate by a factor of 8.[26] Thus, shear thinning in the coacervate would improve its flow through the pores, whereas immature coacervate mixtures with shear thickening would effectively clog the pores.

Once positioned on a solid surface, the coacervates in all mixing ratios exhibit a very high friction coefficient (1.2–1.4, Fig. 6), which would serve to prevent slippage of the foot-to-surface contact in mussels, for example. Indeed, one of us (J. H. Waite, unpublished observation) has lifted a 150 g mussel attached by the tip of its foot (contact area 7 mm^2) to a glass plate of equal weight completely out of the water with no sign of slippage. The observed friction coefficient for the coacervate exceeds that of rubber on dry asphalt [http://www.engineeringtoolbox.com/friction-coefficients-d_778.html].

Finally, coacervates exhibit extraordinarily low interfacial energies with water. A comparison based on mica surfaces is appropriate. The interfacial energy of freshly cleaved mica in water is 107 mJ m^{-2}; addition of an amphiphilic surfactant (lauryl acid) that coats the mica surface reduces it to 8 mJ m^{-2}.[27] A coacervate consisting of two polar polyelectrolytes - HA and fp-151-RGD - effectively decreases interfacial energy to <1 mJ m^{-2}. The low interfacial energy of coacervates (~0.1 mJ m^{-2}) has recently been confirmed by another group using atomic force microscopy.[28] These results bode well for the future of coacervates in wet adhesion, since favorable adhesive spreading over surfaces is a fundamental requirement of good adhesion – in water as well as out.[29]

Notably, the addition of DOPA to the recombinant adhesive protein did not detectably perturb its phase separation, viscosimetric, interfacial or frictional behavior under the conditions tested. This expectation, however, cannot be reliably extended to oxidizing or high pH conditions that lead to DOPA oxidation and formation of DOPA derived cross-links.[2,6]

Conclusion

The surface forces apparatus and microscopic techniques were used to examine the nanostructure, viscosity, friction, and interfacial energy of a mussel-inspired coacervate formed by mixing a recombinant mussel adhesive protein with hyaluronic acid (HA). Dynamic viscosity and cryo-TEM both detect a significant structural transition that coincides with the optimal mixing ratio for coacervation of recombinant mussel adhesive protein with HA. The shear-thinning viscosity, high friction coefficient (>1.2), and low interfacial energy (<1 mJ m^{-2}) of the optimum coacervate provide intriguing engineering insights for the development of future wet adhesive and coating technologies.

Supplementary Material

Refer to Web version on PubMed Central for supplementary material.

Acknowledgments

This work was supported by the National Science Foundation under Grants DMR-07-10521 (Materials World Network) and DMR05-20415 (MRSEC Program), the National Institutes of Health under Grant R01-DE018468, and an Otis Williams fellowship (DSH) in Bioengineering from the Santa Barbara Foundation. We thank Prof. H. J. Cha (POSTECH) and Kollodis Biosciences for providing recombinant mussel adhesive protein samples.

Notes and References

1. Waite JH, Holten-Andersen N, Jewhurst S, Sun CJ. J. Adhes. 2005; 81:297–317.
2. Lee H, Scherer NF, Messersmith PB. Proc. Natl. Acad. Sci. U. S. A. 2006; 103:12999–13003. [PubMed: 16920796]
3. Lee H, Lee BP, Messersmith PB. Nature. 2007; 448:338–341. [PubMed: 17637666]
4. Shao H, Bachus KN, Stewart RJ. Macromol. Biosci. 2009; 9:464–471. [PubMed: 19040222]
5. Westwood G, Horton TN, Wilker JJ. Macromolecules. 2007; 40:3960–3964.
6. Zhao H, Sun CJ, Stewart RJ, Waite JH. J. Biol. Chem. 2005; 280:42938–42944. [PubMed: 16227622]
7. Stewart RJ, Weaver JC, Morse DE, Waite JH. J. Exp. Biol. 2004; 207:4727–4734. [PubMed: 15579565]
8. Bungenberg de Jong HG. Protoplasma. 1932; 15:110–173.
9. Bungenberg de Jong, HG. Complex colloid systems. In: Kruyt, HR., editor. Colloid Science. Elsevier, Amsterdam; 1949. p. 335-400.
10. de Kruif CG, Weinbreck F, de Vries R. Curr. Opin. Colloid Interface Sci. 2004; 9:340–349.
11. Srivastava A, Waite JH, Stucky GD, Mikhailovsky A. Macromolecules. 2009; 42:2168–2176. [PubMed: 20808713]
12. Kausik R, Srivastava A, Korevaar PA, Stucky G, Waite JH, Han S. Macromolecules. 2009; 42:7404–7412. [PubMed: 20814445]
13. Hwang DS, Waite JH, Tirrell M. Biomaterials. 2010; 31:1080–1084. [PubMed: 19892396]
14. Hwang DS, Sim SB, Cha HJ. Biomaterials. 2007; 28:4039–4046. [PubMed: 17574667]
15. Taylor SW. Anal. Biochem. 2002; 302:70–74. [PubMed: 11846377]
16. Luengo G, Schmitt FJ, Hill R, Israelachvili JN. Macromolecules. 1997; 30:2482–2494.
17. Israelachvili JN, Adams GE. J. Chem. Soc., Faraday Trans. 1. 1978; 74:975–1001.
18. O'Neill ME. Mathematika. 1967; 14:170–172.
19. O'Neill ME, Stewartson K. J. Fluid Mech. 1967; 27:705–724.
20. Zeng H, Maeda N, Chen NH, Tirrell M, Israelachvili JN. Macromolecules. 2006; 39:2350–2363.
21. Israelachvili JN. J. Colloid Interface Sci. 1973:44–259.
22. Israelachvili, JN. Surfactants in solution. Milttal, KL.; Bothorel, P., editors. New York: Plenum; 1987. p. 3-33.
23. Israelachvili JN. Colloids Surf., A. 1994; 91:1–8.
24. Vovelle J. Arch. Zool. Exp. Gen. 1965; 106:1–187.
25. Tamarin A, Lewis P, Askey J. J. Morphol. 1976; 149:199–221. [PubMed: 933173]
26. Vogel, S. Life's Devices: The Physical World of Animals and Plants. Princeton: Princeton University Press; 1988.
27. Bailey AI, Price AG, Kay SM. Spec. Discuss. Faraday Soc. 1970; 1:118–127.
28. Spruijt E, Sprakel J, Martien A, Cohen Stuart A, van der Gucht J. Soft Matter. 2010; 6:172–178.
29. Schonhorn, H. Adhesion and Cellulosic and Wood-based Composites. New York: Plenum; 1981. p. 91-111.

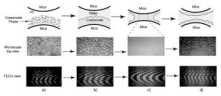

Fig. 1.

Schematic, microscopic top- and FECO views of the adhesion experiment: column (a) HA and fp-151-RGD mixtures settling onto a mica surface, (b) formation of uniform coacervate film on mica surface, (c) spreading and formation of a uniform coacervate bridge between two mica surfaces, (d) after separation and breakage of the coacervate neck.

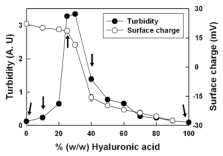

Fig. 2.

Coacervation of hyaluronic acid (HA) and recombinant mussel protein (fp-151-RGD) mixtures. The yield of phase-separated coacervate is indicated by turbidity (●) and surface charge of coacervates as indicated by the zeta potential (○) HA:fp-151-RGD ratios at which viscosity was measured by the SFA (indicated by arrows). Each point represents the average of duplicate measurements.

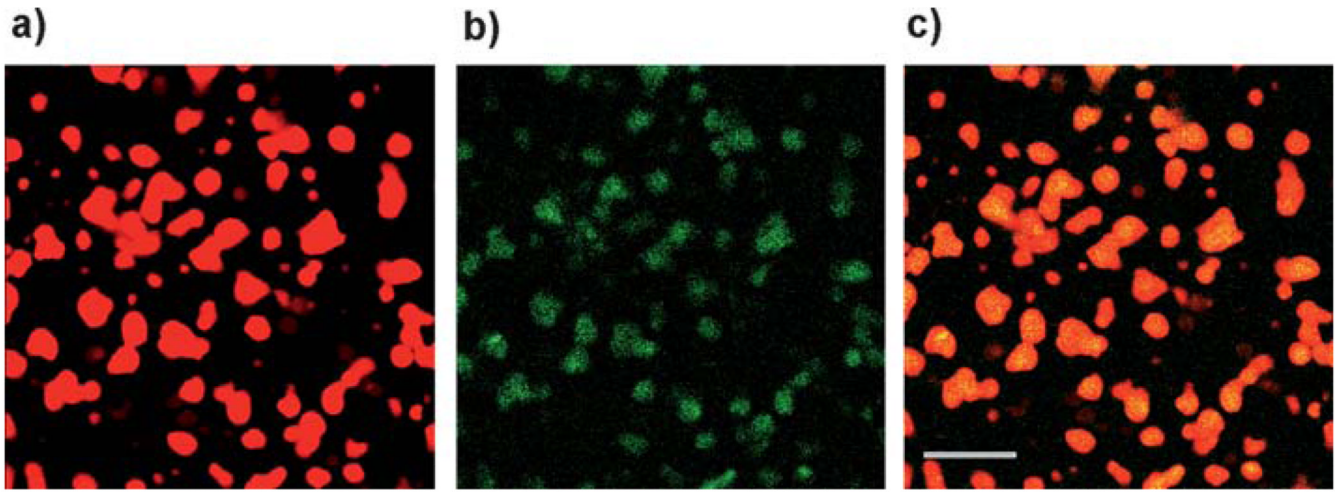

Fig. 3.
Confocal micrographs of a HA/fp-151-RGD coacervate (1 : 3). Rhodamine B-labeled fp-151-RGD emits red (a) while Fluorescein-labeled emits green (b). The image in (c) is the overlap of the two images. The scale bar is 10 μm.

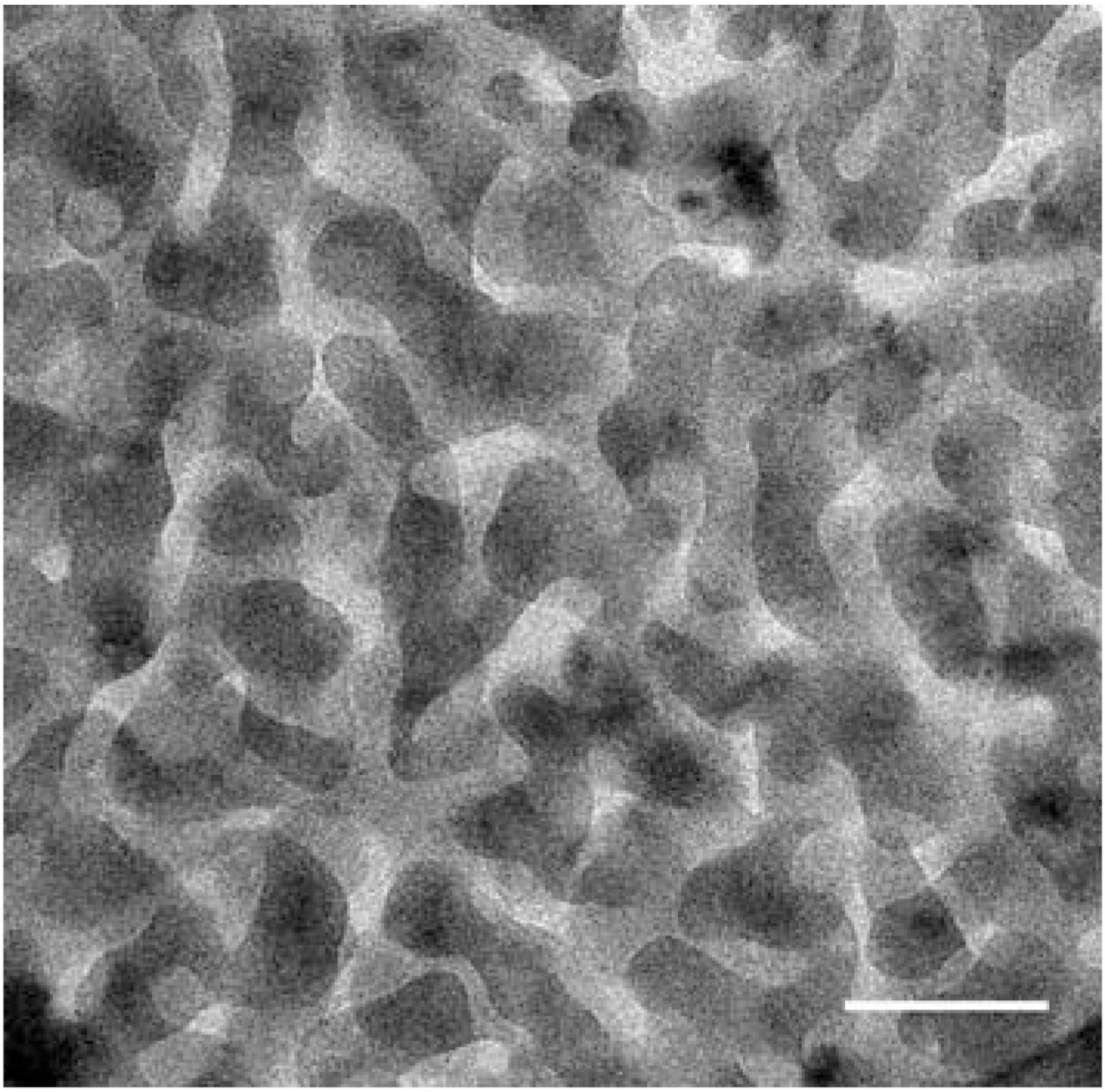

Fig. 4.
Cryo transmission electron microscopy of HA: fp-151-RGD mixing ratios of 1 : 3. The scale bar is 100 nm.

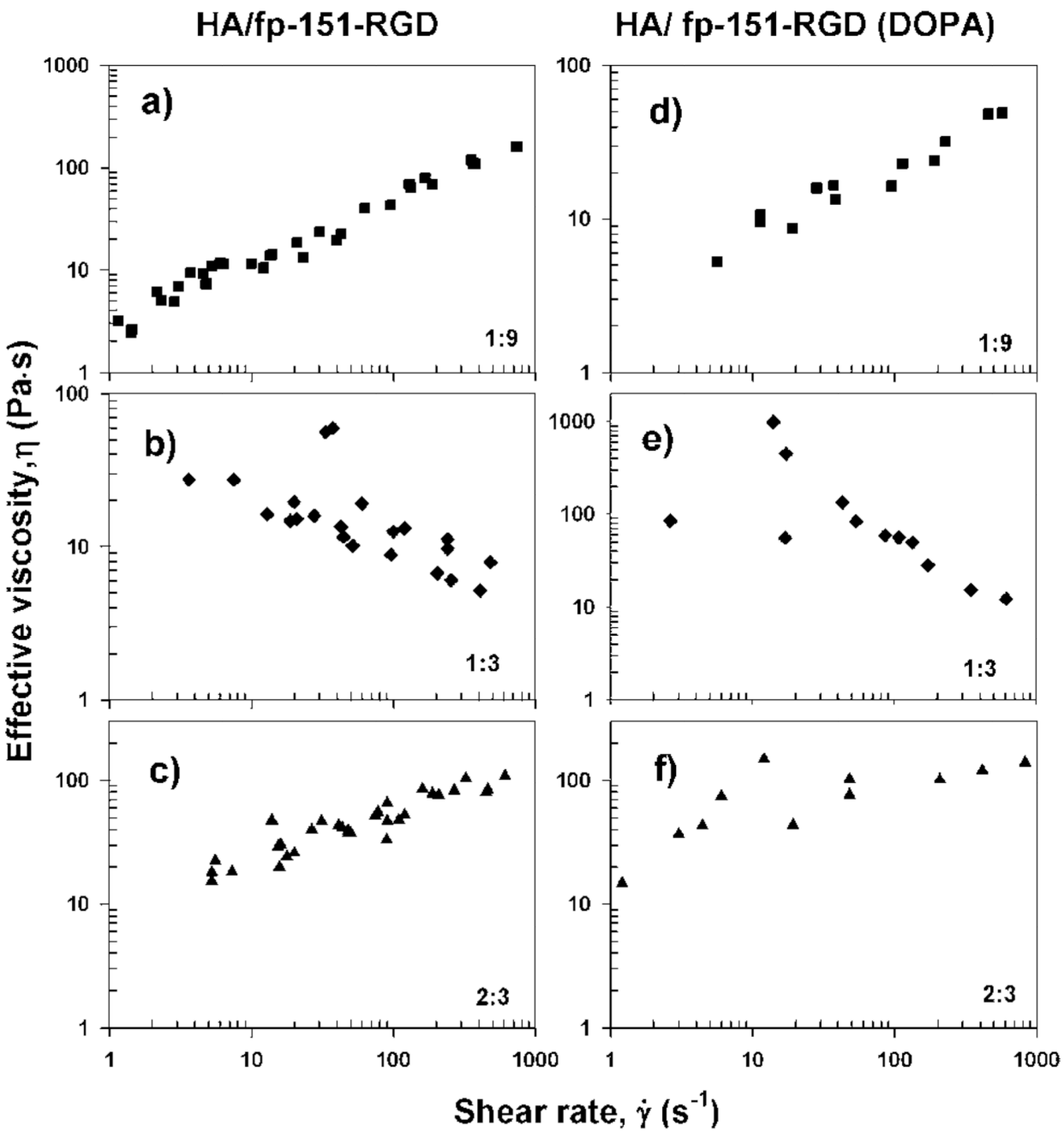

Fig. 5.

Viscosities of coacervates depend on shear rate and mixing ratio of HA with fp-151-RGD and fp-151-RGD (DOPA). HA:fp-151-RGD (a, b, c without DOPA) and HA:fp-151-RGD(DOPA) (d, e, f with DOPA group) HA:fp-151-RGD ratio of (a) 1 : 9, (b) 1 : 3, (c) 2 : 3 (w/w). HA:fp-151-RGD (DOPA) ratio of (d)1 : 9, (e)1 : 3, (f) 2 : 3 (w/w).

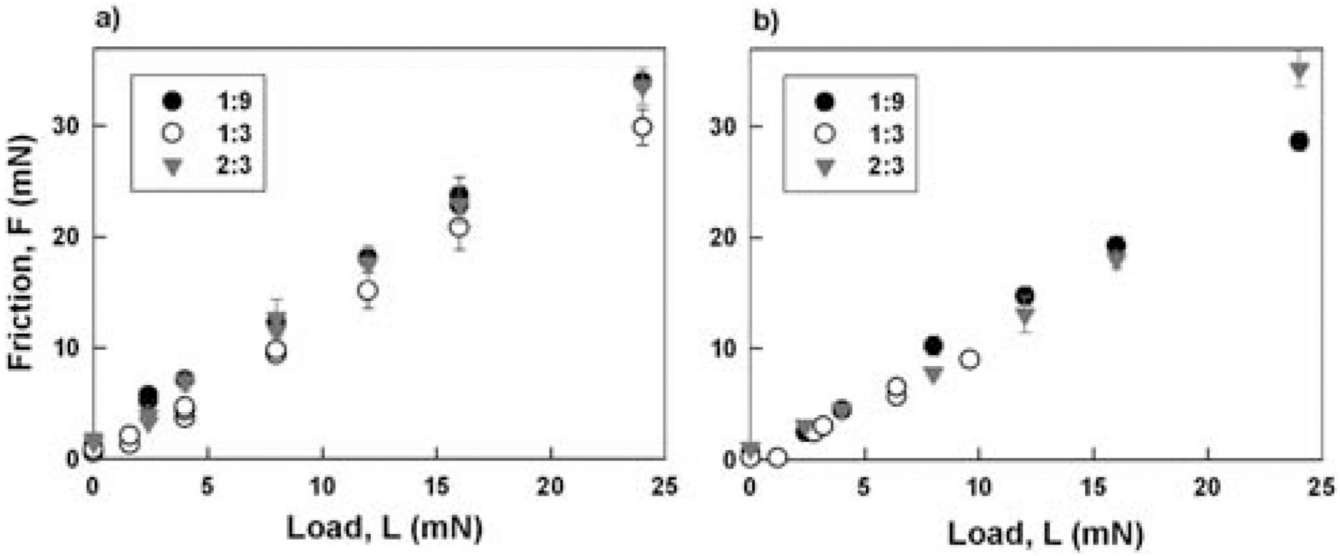

Fig. 6.

Friction *vs*. applied load for HA and fp-151-RGD coacervates at three different mixing ratios (1 : 9, 1 : 3, and 2 : 3), (a) without DOPA, and (b) with DOPA.